IEEE Access
Multidisciplinary ⋮ Rapid Review ⋮ Open Access Journal

Received August 3, 2020, accepted August 24, 2020, date of publication August 26, 2020, date of current version September 10, 2020.

Digital Object Identifier 10.1109/ACCESS.2020.3019757

On the Excitation of Magnetic Current Surface Waves in Truncated Periodic Arrays of Slots Under Extraordinary Transmission Conditions

MIGUEL CAMACHO[1], (Member, IEEE), VICENTE LOSADA[2], RAFAEL R. BOIX[3], (Member, IEEE), AND FRANCISCO MEDINA[3], (Fellow, IEEE)

[1]Department of Electrical and Systems Engineering, University of Pennsylvania, Philadelphia, PA 19104-6390, USA
[2]Department of Applied Physics I, E.T.S. de Ingeniería Informática, University of Seville, 41012 Seville, Spain
[3]Department of Electronics and Electromagnetism, College of Physics, University of Seville, 41012 Seville, Spain

Corresponding author: Miguel Camacho (mcamagu@seas.upenn.edu)

This work was supported by the "Junta de Andalucía" under Grant P12-TIC-1435, and in part by the Ministerio de Ciencia, Innovación y Universidades under Grant TEC2017-84724-P.

ABSTRACT In this paper, we explore the excitation of magnetic current surface waves in truncated periodic arrays of slots in a conducting screen. A specialized Method of Moments (MoM) implementation is presented, which makes it possible to efficiently solve the scattering problem involving truncated arrays of several thousands of slots. By making use of the dispersion diagrams of surface waves propagating along infinite periodic arrays of slots, we are able to explain the absence of magnetic current surface waves in the arrays at frequencies in the neighborhood of the transmission peak associated to the slots natural resonances (length roughly equal to half the wavelength), while they are present when the arrays are excited under extraordinary transmission (EOT) conditions. In order to experimentally check this different behavior, an aluminium plate periodically perforated with slots has been fabricated and fed by means of a pyramidal horn, and the electric field behind the plate has been measured with a planar near-field system at a few centimeters from the plate. Our experimental results and MoM simulations agree, demonstrating the presence of a standing wave pattern of magnetic current surface waves at the EOT frequency, and the absence of surface waves at the slots natural resonant frequency.

INDEX TERMS Extraordinary transmission, arrays, moment methods, periodic structures, scattering.

I. INTRODUCTION

In a seminal paper published in 1998, Ebbesen *et al.* discovered that periodic arrays of small apertures present a transmission coefficient as large as unity at a narrow band of frequencies well-below the expected resonance associated with the size of the apertures [1]. This phenomenon was called Extraordinary Optical Transmission (EOT) since it was first detected at optical frequencies. The first theories for EOT relied on the plasmonic behaviour of metals at optical frequencies [2], although it was not long before several researchers found similarly remarkable EOT for hole arrays at millimeter wave frequencies, where metals can be treated as perfect conductors [3], [4]. Finally, it was accepted that EOT can be explained in terms of the excitation of surface waves (not necessarily surface plasmons) in periodically structured conductor surfaces [5], which is a concept well-known by antenna engineers [6].

In 2000 Neto *et al.* studied the effects introduced by truncations on the distribution of magnetic currents on arrays of slots [7]. At the frequency for which the slots were resonant (length equal to a half a wavelength), the authors found the magnetic currents to be not very different from those obtained in the case of infinite arrays of slots (see [7, Fig. 4.a]), except for the slots located at the boundaries of the truncated arrays where edge effects were stronger. Similar results were obtained for truncated arrays of resonant dipoles in [8, Fig. 1.3.b], and again for truncated arrays of resonant slots in [9, Fig.11]. However, in a series of papers published in 2001 and 2002 [10]–[12], and in a book published in 2003 [8], Munk and collaborators found that bound current surface waves may propagate along truncated metallic arrays of dipoles. These surfaces waves exist at frequencies well-below the resonant frequency of the dipoles

The associate editor coordinating the review of this manuscript and approving it for publication was Santi C. Pavone.

(typically between 20% and 30% below). Recently, Camacho *et al.* [9] found that magnetic current surface waves, similar to those observed by Munk, also appear in truncated arrays of slots at the frequency of EOT, and in this latter case, the wavelength of the surface waves is extremely large [9, Fig. 13]. Also, whereas the electric current surface waves observed in [8], [10]–[12] appear for oblique incidence under plane wave illumination, the magnetic current surface waves of [9] are excited even for normal incidence.

In this paper we study the excitation of magnetic current surface waves in a truncated periodic array of slots under both plane wave and pyramidal horn illuminations. Since the MoM analysis of truncated arrays of slots under plane wave illumination has been described in detail in [9, Section III], in Section II we briefly describe the extension of the MoM analysis of [9] for the case in which the feed is a pyramidal horn, this being a much more realistic scenario. In Section III we use the MoM analysis to show that magnetic current surface waves appear at frequencies well below the resonant frequency of the slots but do not appear at the resonant frequencies of the slots [8], [10]–[12], and that they are present at the frequency of the EOT transmission peak [9]. This difference in behavior is explained by using the dispersion relation of the surfaces waves propagating along the periodic array when it is assumed to be infinite. Also, in Section III we validate our MoM results for pyramidal horn illumination with measurements, and these results show the absence of magnetic current surface waves at the resonant frequency of the slots and the presence of these waves at the frequency of the EOT transmission peak.

The results presented here can pave the way for novel focusing platforms with application in lens and transmitarray antennas and could also be extended for their application at optical frequencies, where the large electric field enhancement achieved on the surface of the array could be exploited for non-linear phenomena.

II. MoM ANALYSIS FOR PYRAMIDAL HORN FEED

Let us consider the problem depicted in Fig. 1, which shows a conducting screen of negligible thickness containing a truncated periodic array of $M = N \times N$ rectangular cells of dimensions $a \times b$. The conducting screen will be assumed to be a perfect electric conductor (PEC). Each of the screen periodic cells includes a rectangular slot of dimensions $w \times l$ occupying a surface η_i $(i = 1, \ldots, M)$. The conducting screen is illuminated by a pyramidal horn antenna with rectangular aperture of dimensions $a_F \times b_F$ $(a_F > b_F)$, the distance between the phase center of the horn antenna and the screen being d_{cF} as shown in Fig. 1. If we assume a time dependence of the type $e^{j\omega t}$ that will be suppressed throughout, the electric field radiated by the horn in the far-field region can be modelled as [13]

$$\mathbf{E}^{\text{inc}}(r_F, \theta_F, \phi_F) = jA_0 \frac{k_0}{2\pi r_F} e^{-jk_0 r_F} \left[C_E(\theta_F) \cos\phi_F \hat{\boldsymbol{\theta}}_F - C_H(\theta_F) \sin\phi_F \hat{\boldsymbol{\varphi}}_F \right] \quad (1)$$

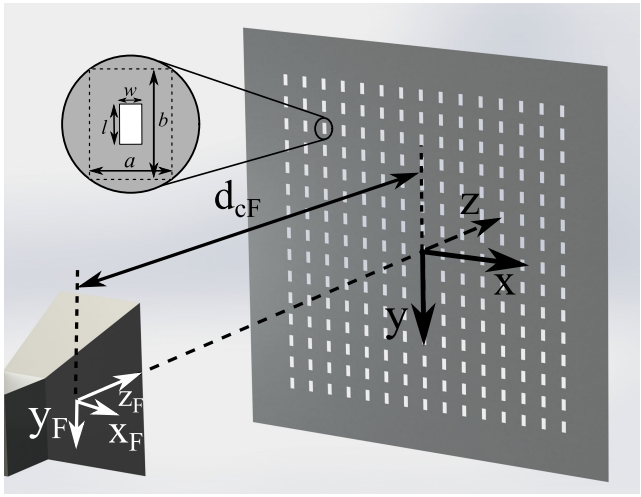

FIGURE 1. Pyramidal horn illuminating a conducting screen containing a periodic array of slots. Two coordinates systems are used, $\{x_F, y_F, z_F\}$ with origin at the phase center of the horn, and $\{x, y, z\}$ with origin at the center of the screen.

where $k_0 = \omega\sqrt{\mu_0\epsilon_0} = 2\pi/\lambda_0$, and where

$$C_E(\theta_F) = \cos^{q_E}\theta_F \quad (2)$$

$$C_H(\theta_F) = \cos^{q_H}\theta_F \quad (3)$$

The coordinates $\{r_F, \theta_F, \phi_F\}$ of (1) to (3) are spherical coordinates relative to the coordinate system with origin at the phase center of the horn (see Fig. 1). The value of q_E can be estimated for a particular pyramidal horn by carrying out a logarithmic least squares fit of the main beam of the normalized radiation pattern of the horn to (2) in the E plane. A similar fit of the main beam of the normalized radiation pattern of the horn to (3) in the H plane enables the determination of q_H. The magnetic field radiated by the horn in the far field can be obtained as $\mathbf{H}^{\text{inc}} = \left(\hat{\mathbf{r}}_F \times \mathbf{E}^{\text{inc}}\right)/Z_0$ $(Z_0 = \sqrt{\mu_0/\varepsilon_0})$.

Let $\mathbf{E}_t^{\text{sc}}(x, y, z = 0)$ be the tangential electric field excited in the M slots of the conducting screen of Fig. 1 by the feeding horn ($\mathbf{E}_t^{\text{sc}}(x, y, z = 0) = \mathbf{0}$ outside the slots since the screen is assumed to be a PEC), and let $\mathbf{M}^{\text{sc}}(x, y) = \hat{\mathbf{z}} \times \mathbf{E}_t^{\text{sc}}(x, y, z = 0)$ be the magnetic current density in the slots. As shown in [9], in order to obtain $\mathbf{E}_t^{\text{sc}}(x, y, z = 0)$ in the M slots η_i $(i = 1, \ldots, M)$, we need to solve the set of M coupled integral equations

$$\mathbf{J}^{\text{as}}(x, y) + \sum_{j=1}^{M} \iint_{\eta_j'} \overline{\mathbf{G}}_M(x - x', y - y') \cdot \mathbf{E}_t^{\text{sc}}(x', y', z = 0)\, dx'dy' = \mathbf{0} \quad (x, y) \in \eta_i \quad (i = 1, \ldots, M) \quad (4)$$

where the dyadic Green's function $\overline{\mathbf{G}}_M(x, y)$ is defined in [9, Eqns. (2)-(3)], and $\mathbf{J}^{\text{as}}(x, y)$ is the electric current density that would be generated on the conducting screen by the feeding horn in the absence of the slots (which is generated by the horn itself and by its image through the conducting screen). Since $\mathbf{J}^{\text{as}}(x, y)$ does not appreciably vary within η_i

$(i = 1, \ldots, M)$, we can assume that $\mathbf{J}^{\text{as}}(x, y)$ is constant within η_i and equal to the value of this function at the center point of η_i of coordinates $(x = x_{ci}, y = y_{ci}, z = 0)$. Therefore, if $\mathbf{J}^{\text{as}}(x = x_{ci}, y = y_{ci}) = \mathbf{J}_i^{\text{as}}$, (4) can be approximately rewritten as

$$\mathbf{J}_i^{\text{as}} + \sum_{j=1}^{M} \iint_{\eta_j'} \overline{\mathbf{G}}_M(x - x', y - y') \cdot \mathbf{E}_t^{\text{sc}}(x', y', z = 0)\, dx'dy' = \mathbf{0} \quad (x, y) \in \eta_i \quad (i = 1, \ldots, M) \tag{5}$$

It can be shown that $\mathbf{J}_i^{\text{as}}$ is given by

$$\mathbf{J}_i^{\text{as}} = \frac{\text{j}A_0 k_0}{\pi r_{Fi} Z_0} \text{e}^{-\text{j}k_0 r_{Fi}} \Big[\Big\{ C_E(\theta_{Fi}) \cos^2\phi_{Fi} + C_H(\theta_{Fi}) \times \sin^2\phi_{Fi} \cos\theta_{Fi} \Big\} \hat{\mathbf{x}} - \{ -C_E(\theta_{Fi}) \sin\phi_{Fi} \cos\phi_{Fi} + C_H(\theta_{Fi}) \sin\phi_{Fi} \cos\phi_{Fi} \cos\theta_{Fi} \} \hat{\mathbf{y}} \Big] \tag{6}$$

where $r_{Fi} = \sqrt{(x_{ci})^2 + (y_{ci})^2 + (d_{cF})^2}$, $\cos\theta_{Fi} = d_{cF}/\sqrt{(x_{ci})^2 + (y_{ci})^2 + (d_{cF})^2}$, $\cos\phi_{Fi} = x_{ci}/\sqrt{(x_{ci})^2 + (y_{ci})^2}$ and $\sin\phi_{Fi} = y_{ci}/\sqrt{(x_{ci})^2 + (y_{ci})^2}$.

In order to solve the set of M integral equations of (5), $\mathbf{E}_t^{\text{sc}}(x, y, z = 0)$ has to be expressed as a linear combination of known basis functions $\mathbf{d}_{jl}(x, y)$ in the M slots as shown below

$$\mathbf{E}_t^{\text{sc}}(x, y, z = 0) \approx \sum_{l=1}^{N_b} e_{jl} \mathbf{d}_{jl}(x, y) \quad (x, y) \in \eta_j \tag{7}$$

In this paper Chebyshev polynomials weighted by an edge condition term have been chosen for the basis functions $\mathbf{d}_{jl}(x, y)$ (see [9, Eqns. (29)-(39) & Eqns. (52)-(56)]). After substituting (6) into (5) and applying Galerkin's version of MoM, a system of linear equations for the unknown coefficients e_{jl} is obtained. The solution of this system of equations makes it possible to determine the magnetic current density, $\mathbf{M}^{\text{sc}}(x, y)$, in the slots. As shown in [9], the use of basis functions that account for the singular behavior of the fields at the slot edges guarantees a fast convergence of MoM with respect to the number of basis functions (see [9, Fig. 6]). Also, very sophisticated analytical techniques have been developed for the efficient computation of the MoM matrix entries when these basis functions are employed (see [9, Section III]), which enables the analysis of screens with several thousands of slots within a few seconds of CPU time in a laptop computer.

A dimensionless transmission coefficient through the perforated screen, T, can be defined as the ratio between the power radiated by the slots into the $z > 0$ half plane, P_{rad}, and the power radiated by the horn that is available at the surface occupied by the M slots, P_{av}, i. e.,

$$T = \frac{P_{\text{rad}}}{P_{\text{av}}} \tag{8}$$

where

$$P_{\text{av}} = \frac{1}{2}\text{Re}\left\{ \int_{-Na/2}^{+Na/2} \int_{-Nb/2}^{+Nb/2} \left[\mathbf{E}^{\text{inc}} \times (\mathbf{H}^{\text{inc}})^* \right] \cdot \hat{\mathbf{z}} dydx \right\} \tag{9}$$

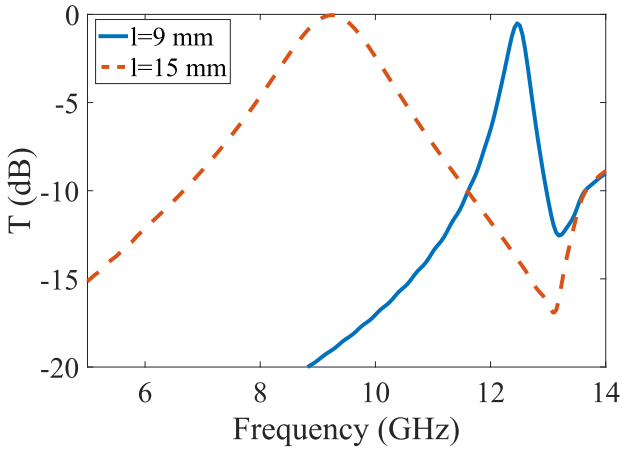

FIGURE 2. **Frequency dependent transmission coefficient for two different truncated arrays of slots. The arrays are illuminated by a plane wave under normal incidence. Parameters: $a = b = 22.5$ mm, $l = 15$ mm (dashed line) and $l = 9$ mm (solid line), $w = 3$ mm, $M = 1600$.**

After some manipulations, it can be shown that P_{rad} can be determined as

$$P_{\text{rad}} = \frac{1}{2}\text{Re}\left\{ \sum_{i=1}^{M} \int\int_{\eta_i} \left[\mathbf{E}_t^{\text{sc}}(x, y, z = 0) \times (\mathbf{H}_t^{\text{sc}}(x, y, z = 0))^* \right] \cdot \hat{\mathbf{z}} dydx \right\} = -\frac{1}{4}\text{Re}\left\{ \sum_{i=1}^{M} \sum_{j=1}^{M} \sum_{k=1}^{N_b} \sum_{l=1}^{N_b} e_{ik} (\Delta_{ij}^{kl})^* e_{jl}^* \right\} \tag{10}$$

where the coefficients e_{jl} have been introduced in (7), and Δ_{ij}^{kl} are the MoM matrix entries defined in [9, Eqns. (39) & (43)]. Owing to the definition given in (8), the transmission coefficient T will always be smaller (or at most, equal) than one in natural units.

Once the set of integral equations of (4) has been solved and the tangential electric field at the conducting screen, $\mathbf{E}_t^{\text{sc}}(x, y, z = 0)$, is known, the tangential electric field at a plane parallel to the screen, placed at a distance h_p of the screen in the region $z > 0$, can be obtained as

$$\mathbf{E}_t^{\text{sc}}(x, y, z = h_p) = \frac{1}{4\pi^2} \int_{-\infty}^{+\infty} \int_{-\infty}^{+\infty} \widetilde{\mathbf{E}}_t^{\text{sc}}(k_x, k_y, z = 0) \times \text{e}^{\text{j}(k_x x + k_y y)} \text{e}^{-\sqrt{k_x^2 + k_y^2 - k_0^2} h_p} dk_x dk_y \tag{11}$$

where $\widetilde{\mathbf{E}}_t^{\text{sc}}(k_x, k_y, z = 0) \approx \sum_{j=1}^{M} \sum_{l=1}^{N_b} e_{jl} \widetilde{\mathbf{d}}_{jl}(k_x, k_y)$ is the 2-D Fourier transform of $\mathbf{E}_t^{\text{sc}}(x, y, z = 0)$ ($\widetilde{\mathbf{d}}_{jl}(k_x, k_y)$ is the 2-D Fourier transform of $\mathbf{d}_{jl}(x, y)$). The integrals of (11) can be comfortably carried out for a sufficiently large number of samples of x and y at the plane $z = h_p$ by means of the FFT algorithm. This computation makes it possible to compare the simulated values of $\mathbf{E}_t^{\text{sc}}$ at the plane $z = h_p$ with the values of $\mathbf{E}_t^{\text{sc}}$ measured at this plane by means of an open waveguide probe.

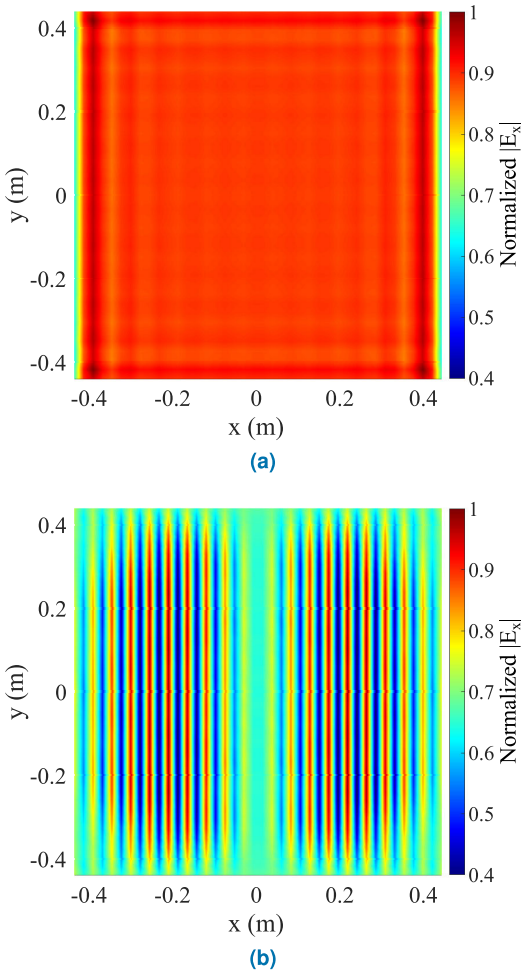

FIGURE 3. Magnitude of $|\mathbf{E}_t^{sc}(x, y, z = 0) \cdot \hat{\mathbf{x}}|$ (dominant component of the transverse electric field at the conducting screen) for one of the truncated periodic array of slots studied in Fig. 2 -case $l = 15$ mm- at (a) 9.3 GHz and (b) 6 GHz. The numerical values are normalized to the maximum. Plane wave illumination under normal incidence is assumed. Parameters: $a = b = 22.5$ mm, $w = 3$ mm, $M = 1600$.

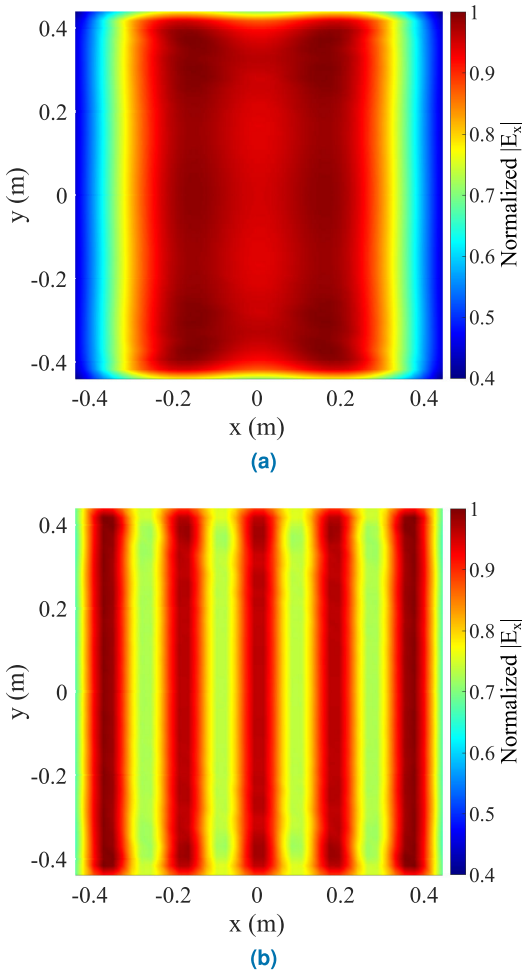

FIGURE 4. Magnitude of $|\mathbf{E}_t^{sc}(x, y, z = 0) \cdot \hat{\mathbf{x}}|$ (dominant component of the transverse electric field at the conducting screen) for one of the truncated periodic array of slots studied in Fig. 2 -case $l = 9$ mm- at (a) 12.4 GHz and (b) 11.4 GHz. The numerical values are normalized to the maximum. Plane wave illumination under normal incidence is assumed. Parameters: $a = b = 22.5$ mm, $w = 3$ mm, $M = 1600$.

III. RESULTS AND DISCUSSION

Fig. 2 shows the transmission coefficient of two periodic truncated arrays of slots when the array is illuminated by a plane wave under normal incidence. This transmission coefficient can be obtained, either by introducing the results of the MoM formulation of [9] into Eqns. (8) to (10), or by using the MoM formulation of Section II and taking a sufficiently large value of d_{cF}. The dashed line corresponds to an array with a slot length of $l = 15$ mm, i. e., $l > a/2$, which is within the range of values usually employed in frequency selective surfaces (FSSs) to allocate a band pass filter before the onset of grating lobes [4]. Note the presence of a transmission peak at roughly 9.3 GHz when the slots are resonant (length roughly equal to half the wavelength). The solid line corresponds to an array with a slot length of $l = 9$ mm, i. e., $l < a/2$. In this latter case, there is an EOT peak at 12.4 GHz below the Wood's anomaly (onset of grating lobes) at 13.3 GHZ, and the slots resonate individually at a frequency above the onset of grating lobes [4].

Figs.3(a) and (b) show the distribution of magnetic currents obtained for the truncated periodic array with longer slots studied in Fig. 2 at 9.3 GHz (resonant frequency of the slots) and 6 GHz respectively. Note that the distribution is very smooth at the resonant frequency of the slots, 9 GHz, except for some edge effects of the type predicted in [7]. To find the excitation of a couple of surface waves of magnetic currents along the x direction, one needs to go as low as 6 GHz, well below the resonant frequency of the slots, as predicted by Munk [8]. In contrast, Figs.4(a) and (b) show the distribution of magnetic currents for the case of a truncated periodic array with shorter slots studied in Fig. 2. The results of Figs.4(a) and (b) are obtained at 12.4 GHz (EOT frequency) and 11.4 GHz. At both frequencies, we find a standing surface wave pattern of magnetic currents along the x direction, but the wavelength of the surface waves excited is substantially larger at the EOT frequency, in agreement with the results of [9]. Following [11] and [12], we have computed the discrete spatial Fourier transform of the magnetic currents

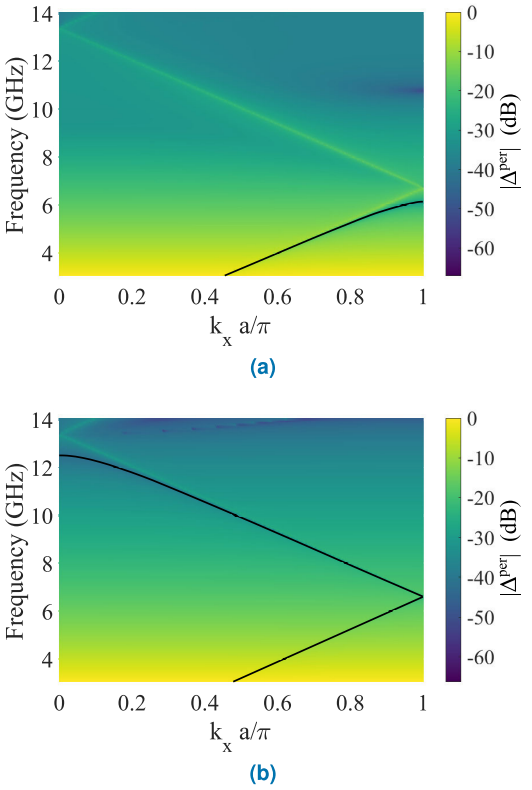

FIGURE 5. Black solid lines represent the real-plane projection of the complex dispersion relation for the surface waves supported by the periodic arrays of slots studied in Fig. 2 when they are assumed to be infinite (non-truncated). (a) is for the case $l = 15$ mm and (b) is for the case $l = 9$ mm. The colormap in the background represents the absolute value of the determinant of the MoM matrix, which turns out to be minimum at the position of the black solid lines. Parameters: $a = b = 22.5$ mm, $w = 3$ mm.

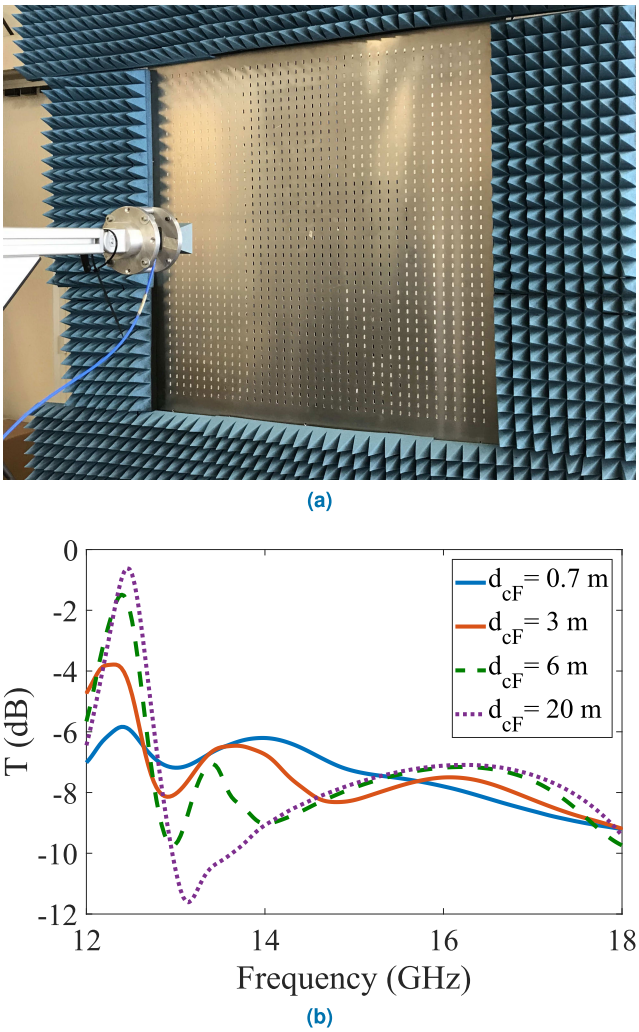

FIGURE 6. (a) Experimental setup showing the finite periodic array of slots illuminated by a Narda 639 standard gain horn antenna. The array of slots is surrounded by absorbing material. Behind the conducting screen, the electric field distribution is measured at a distance h_p by using an open-waveguide near-field probing system. (b) Transmission through the conducting screen in the Ku-band for different values of the distance between the phase center of the horn and the conducting screen, d_{cF}. Parameters: $a = b = 22.5$ mm, $l = 9$ mm, $w = 3$ mm, $M = 1600$.

in Figs. 3(b) and 4(b) and we have obtained three peaks, one corresponding to the so-called Floquet current (with zero wavenumber in this case since normal incidence is assumed), and the other two corresponding to surface waves propagating along the x axis in oppposite directions (see [11, Fig. 1] and [12, Fig.2]). When these three currents are isolated and combined, one obtains a sinusoidal function on a pedestal (the pedestal being due to the Floquet current, i.e. non-truncated solution), and the distance between maxima provides the wavelength of the magnetic current surface waves. This implies that the wavelength (distance between maxima) of the surface waves shown in Fig. 3(b) is roughly 47.5 mm, and that the wavelenght of the surface waves shown in Fig. 4(b) is roughly 180 mm.

Although here we restrict our study to the excitation of the aforementioned magnetic current surface waves at normal incidence, one would expect that an obliquely incident plane wave would break the mirror symmetry of the excitation of the pair of surface waves, i.e., the two counter-propagating surface waves would be excited with different amplitudes, plus the non-truncated solution would also consist on a Floquet-wave solution with phasing constant along the surface different than zero. In sum, one would obtain a non-symmetric electric field distribution on the surface of the array, which could lead to interesting field concentrations and which will be subject of further study elsewhere.

In order to justify the results of Figs. 3 and 4, we have obtained the complex propagation constants for the surface waves that can propagate along the x direction of the arrays studied in Fig. 2 when they are assumed to be infinite. These propagation constants can be obtained as the zeros of the determinant of the MoM matrix of the infinite periodic problem for a prescribed frequency. For details concerning the numerical computation of these propagation constants, please refer to [14]. Figs. 5(a) and (b) show the phase constant (real part of the propagation constant) versus frequency (the so-called dispersion diagram) for the arrays studied in Figs. 3 and 4 respectively. In the case of Fig. 5(a), note that surface waves can propagate for frequencies below 6.5 GHz

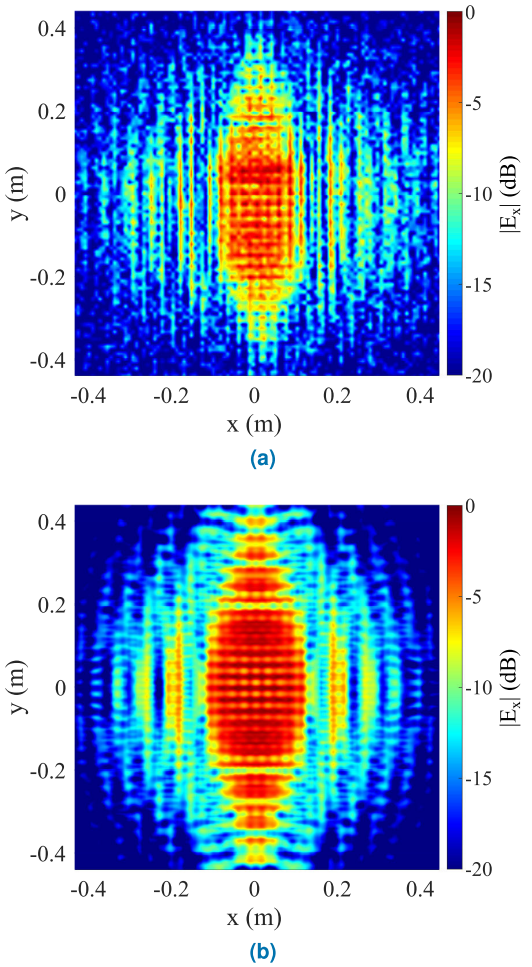

FIGURE 7. (a) Experimental and (b) numerical values of $|\mathbf{E}_t^{sc}(x, y, z = h_p) \cdot \hat{\mathbf{x}}|$ (dominant component of the transverse electric field transmitted by the conducting screen at a distance h_p of the screen) at $f = 12.35$ GHz (EOT transmission peak) when the conducting screen is fed by a Narda 639 standard gain horn (see Fig. 6(a)). Parameters: $a = b = 22.5$ mm, $l = 9$ mm, $w = 3$ mm, $d_{cF} = 70$ cm, $h_p = 9$ cm, $M = 1600$.

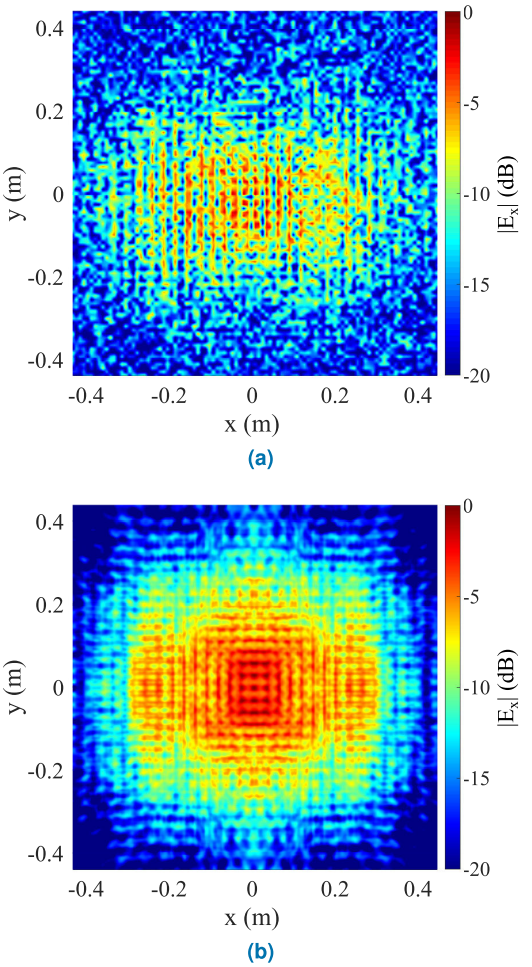

FIGURE 8. (a) Experimental and (b) numerical values of $|\mathbf{E}_t^{sc}(x, y, z = h_p) \cdot \hat{\mathbf{x}}|$ (dominant component of the transverse electric field transmitted by the conducting screen at a distance h_p of the screen) at $f = 16$ GHz (resonant frequency of the slots) when the conducting screen is fed by a Narda 639 standard gain horn (see Fig. 6(a)). Parameters: $a = b = 22.5$ mm, $l = 9$ mm, $w = 3$ mm, $d_{cF} = 70$ cm, $h_p = 8$ cm, $M = 1600$.

but not beyond that frequency, which justifies why surface waves are not present in Fig. 3(a) at 9.3 GHz, whereas a standing surface wave pattern is clearly present in Fig. 3(a) at 6 GHz. In fact, Fig. 5(a) shows the phase constant at 6 GHz is roughly $k_x a/\pi = 0.95$, which corresponds to a bound mode in the infinite periodic structure with wavelength of $\lambda_x = a/0.475 \approx 47.5$ mm, in agreement with the distance between maxima of Fig. 3(b). Concerning Fig. 5(b), one can see the surface waves can propagate for frequencies below 12.5 GHz, which justifies the appearance of a standing wave pattern in both Figs. 4(a) and (b). At the EOT transmission peak, 12.4 GHz, the phase constant is close to zero, which justifies the large wavelength observed in the standing surface wave pattern of Fig. 4(a). This phase constant in the neighborhood of zero indicates the surface wave has become leaky in the infinite periodic structure and radiates in the broadside direction, which is an alternative explanation for the appearance of the EOT phenomenon. Fig. 5(b) shows that the phase constant of the surface waves becomes larger as we decrease frequency, and at a frequency of 11.4 GHz, it is roughly $k_x a/\pi = 0.25$, which corresponds to a wavelength of $\lambda_x = a/0.125 = 180$ mm, again in agreement with the distance between maxima of Fig. 4(b).

To validate the results obtained from the MoM analysis of the truncated periodic arrays, we have performed an experiment in which we have built a periodic array composed of 40×40 slots of length $l = 9$ mm and width $w = 3$ mm, which are cut into a 1.5 mm-thick aluminium plate. This plate is illuminated with a standard-gain horn antenna Narda 639 for Ku-band. To accurately results for such experimental setup, the illumination is introduced into the model as shown in Section II. The experimental setup is shown in Fig. 6(a). A NSI planar near field measurement scanner has been used to measure the tangential electric field at a distance roughly $h_p \approx 4\lambda_0$ behind the screen. Numerical simulations have shown that the electric field distribution at this position can

be used to reliably represent the magnetic currents in the array. Fig.6(b) shows the simulated values of the transmission coefficient defined in (8) as a function of frequency in the Ku-band under the conditions of the experiment for several values of the distance between the horn phase center and the conducting screen, d_{cF}. The results of Fig.6(b) for $d_{cF} = 20$ m practically mimic those of Fig.2 when $l = 9$ mm, showing the EOT peak at 12.4 GHz, and the resonant frequency of the slots at roughly 16 GHz ($l \approx \lambda_0/2$). As the horn approaches the screen, the less uniform the illumination is (the stronger the phase gradient), and the less the transmission is at the EOT peak.

Figs. 7(a) and (b) show the experimental and numerical results obtained for the electric field distribution at the EOT peak within the plane $z = h_p = 9$ cm behind the screen. Good agreement is found between the two sets of results. These results indicate the existence of a standing wave pattern with nodes and antinodes along the x direction, which is in agreement with the results of Fig.4(a). Figs.5(a) and (b) show the experimental and numerical results obtained for the electric field distribution at the resonant frequency of the slots in the plane $z = h_p = 8$ cm behind the screen. Reasonable agreement is found between the two sets of results. Whereas the results of Figs. 7(a) and (b) indicate the existence of a standing wave pattern of surface waves travelling in opposite directions, the results of Figs.8(a) and (b) basically reproduce the radiation pattern of the horn on the other side of the conducting screen. As shown in [8], the current surface waves do not appear at the resonant frequency of the elements used in the unit cells of the truncated periodic array.

IV. CONCLUSION

In this paper we have explored the remarkable differences between the distribution of magnetic currents in truncated periodic arrays of slots in conducting screens at the resonant frequency of the slots, where only edge effects are apparent, and at the EOT frequency, where magnetic current surface waves are excited. For that purpose, a very efficient MoM code has been implemented for the determination of the magnetic currents in the slots when the conducting screen is illuminated by a pyramidal horn antenna. The dispersion relations of the surfaces waves propagating along the arrays when they are assumed to be infinite allow us to show the conditions for the appearance of the magnetic current surface waves in the truncated arrays. The absence of surface waves at the resonant frequency of the slots and the presence of surface waves at the EOT frequency peak have booth been experimentally demonstrated by measuring the electric field distribution behind a slotted conducting screen with a near-field system. Good agreement has been found between the MoM results and experimental results.

REFERENCES

[1] T. W. Ebbesen, H. J. Lezec, H. F. Ghaemi, T. Thio, and P. A. Wolff, "Extraordinary optical transmission through sub-wavelength hole arrays," *Nature*, vol. 391, no. 6668, pp. 667–669, Feb. 1998.

[2] H. F. Ghaemi, T. Thio, D. E. Grupp, T. W. Ebbesen, and H. J. Lezec, "Surface plasmons enhance optical transmission through subwavelength holes," *Phys. Rev. B, Condens. Matter*, vol. 58, no. 11, pp. 6779–6782, Sep. 1998.

[3] M. Beruete, M. Sorolla, I. Campillo, J. S. Dolado, L. Martin-Moreno, J. Bravo-Abad, and F. J. Garcia-Vidal, "Enhanced millimeter wave transmission through quasioptical subwavelength perforated plates," *IEEE Trans. Antennas Propag.*, vol. 53, no. 6, pp. 1897–1903, Jun. 2005.

[4] F. Medina, F. Mesa, and R. Marques, "Extraordinary transmission through arrays of electrically small holes from a circuit theory perspective," *IEEE Trans. Microw. Theory Techn.*, vol. 56, no. 12, pp. 3108–3120, Dec. 2008.

[5] F. J. G. de Abajo, "Colloquium: Light scattering by particle and hole arrays," *Rev. Mod. Phys.*, vol. 79, pp. 1267–1290, no. 4, Oct./Dec. 2007.

[6] C. C. Cutler, "Genesis of the corrugated electromagnetic surface," in *Proc. IEEE Antennas Propag. Soc. Int. Symp. URSI Nat. Radio Sci. Meeting*, vol. 1, Jun. 1994, pp. 1456–1459.

[7] A. Neto, S. Maci, G. Vecchi, and M. Sabbadini, "A truncated floquet wave diffraction method for the full-wave analysis of large phased arrays. II. Generalization to 3-D cases," *IEEE Trans. Antennas Propag.*, vol. 48, no. 4, pp. 601–611, Apr. 2000.

[8] A. Ben Munk, *Finite Antenna Arrays and FSS*. Hoboken, NJ, USA: Wiley-Interscience, 2003, p. 3.

[9] M. Camacho, R. R. Boix, and F. Medina, "Computationally efficient analysis of extraordinary optical transmission through infinite and truncated subwavelength hole arrays," *Phys. Rev. E, Stat. Phys. Plasmas Fluids Relat. Interdiscip. Top.*, vol. 93, no. 6, Jun. 2016, Art. no. 063312.

[10] B. A. Munk, D. S. Janning, J. B. Pryor, and R. J. Marhefka, "Scattering from surface waves on finite FSS," *IEEE Trans. Antennas Propag.*, vol. 49, no. 12, pp. 1782–1793, Dec. 2001.

[11] D. S. Janning and B. A. Munk, "Effects of surface waves on the currents of truncated periodic arrays," *IEEE Trans. Antennas Propag.*, vol. 50, no. 9, pp. 1254–1265, Sep. 2002.

[12] O. A. Civi, P. H. Pathak, P. Janpugdee, and B. A. Munk, "Surface waves on a finite planar dipole array in free space," in *Proc. IEEE Antennas Propag. Soc. Int. Symp.*, San Antonio, TX, USA, Jun. 2002, pp. 78–81, doi: 10.1109/APS.2002.1016032.

[13] Y. T. Lo and S. W. Lee, *Antenna Handbook. Volume I: Antenna Fundamentals and Mathematical Techniques*. New York, NY, USA: Van Nostrand Reinhold, 1993, pp. 28–29.

[14] M. Camacho, R. R. Boix, F. Medina, A. P. Hibbins, and J. R. Sambles, "Theoretical and experimental exploration of finite sample size effects on the propagation of surface waves supported by slot arrays," *Phys. Rev. B, Condens. Matter*, vol. 95, no. 24, Jun. 2017, Art. no. 245425.

MIGUEL CAMACHO (Member, IEEE) was born in Seville, Spain, in 1993. He received the B.Sc. degree from the University of Seville, in 2015, and the Ph.D. degree from the University of Exeter, U.K., in 2019, both in physics.

He is currently a Postdoctoral Fellow with the University of Pennsylvania, Philadelphia, USA. During his undergraduate studies, he was awarded a Student Research Fellowship from the Spanish Ministry of Education, and he was selected to work as a Summer Student with the Deutsches Elektronen-Synchrotron, Hamburg, Germany. He has authored more than ten peer-reviewed journal articles and holds a patent. His research interests include numerical methods for the analysis of electromagnetic scattering by periodic and truncated arrays and the design of non-dispersive metasurfaces with higher symmetries. He has received several awards from Seville's City Hall and the University of Seville for the best academic record of the College of Physics, from 2011–2015. He was also awarded the Spanish Ministry of Education National Award as the Best Physics Undergraduate in the country for the same period. He was a recipient of the IEEE Antennas and Propagation Society Doctoral Grant, in 2017, and the URSI Commission-B Young Scientist Award, in 2019.

VICENTE LOSADA was born in São Paulo, Brazil, in February 1969. He received the Licenciado and Ph.D. degrees in physics from the University of Sevilla, Seville, Spain, in 1992 and 1997, respectively. He has been an Associate Professor with the Department of Applied Physics I, University of Seville, since 2004. His research interests include manufacture and near-field and far-field measurements techniques for antennas. He acts as a Reviewer of the IEEE TRANSACTIONS ON ANTENNAS and PROPAGATION.

RAFAEL R. BOIX (Member, IEEE) received the Licenciado and Ph.D. degrees in physics from the University of Seville, Sevilla, Spain, in 1985 and 1990, respectively.

Since 1986, he has been with the Electronics and Electromagnetism Department, University of Seville, where he became a Tenured Professor, in 2010. His research interests include efficient numerical analysis of periodic planar multilayered structures with applications to the design of frequency selective surfaces, and reflectarray antennas.

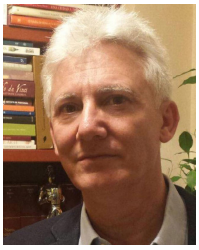

FRANCISCO MEDINA (Fellow, IEEE) was born in Puerto Real, Cádiz, Spain, in 1960. He received the Licenciado and Ph.D. degrees in physics from the Universidad de Sevilla, Seville, Spain, in 1983 and 1987, respectively. He is currently a Professor of electromagnetism with the Department of Electronics and Electromagnetism, Universidad de Sevilla, where he is also the Head of the Microwaves Group. His current research interests include analytical and numerical methods for planar structures, anisotropic materials, artificial media modeling, and planar microwave circuits. He has published a number of book chapters, journal articles, and conference papers on these topics. He is the Editor-in-Chief of the *International Journal of Microwave and Wireless Technologies* and a member of the editorial board of the *International Journal of RF and Microwave Computer-Aided Engineering*.